Research on Secondary Frequency Control Strategy for Islanded Microgrid

Baobing Pang[1,2], Xueli Chen[1,2], Zhenyu Lv[1,2], Cheng Liang[1,2]

[1]School of Electrical and Automation Engineering, Nanjing Normal University,

[2]Nanjing, Jiangsu Province,210042, China

e-mail: 1575088020@qq.com

Abstract. In view of the fact that the primary control has a steady-state frequency difference, this paper aims at the rapidity and economy of isolated microgrid frequency modulation, and proposes a secondary frequency control strategy for islanding microgrid based on distributed control. In order to verify the reliability of the strategy, the correctness and effectiveness of the proposed frequency modulation strategy were verified by Matlab/Simulink simulation analysis.

1. Introduction

Based on the hierarchical control architecture, this paper studies the frequency control method of islanding microgrid from three aspects: distributed power supply, grid-connected converter and microgrid system. In order to overcome the deficiencies of the existing centralized and decentralized control methods, this paper proposes a layered cooperative frequency control strategy that includes primary control and secondary control from the control objectives of the equipment layer and system layer, and realizes the frequency of islanding microgrid and Stability control [1]. Finally, the correctness and effectiveness of the proposed frequency modulation strategy are verified by Matlab/Simulink simulation analysis.

2.The Secondary Control Strategy of Island Microgrid

In order to make up for the voltage deviation and frequency deviation generated in the primary control loop, a secondary control strategy is introduced here. In the secondary control, the amplitude and frequency of the output voltage of the inverter are re-controlled to the primary control signal so that it can be re-balanced to achieve the optimal operation of the system operation.

2.1Economical secondary control principle

Distributed power sources can be broadly classified into three types: internal combustion engine type power supplies, dispatchable power supplies, and unschedulable power supplies. Its power generation cost is determined by many factors, but its cost function can generally be approximated as a quadratic function:

$$C_i(P_i) = \alpha_i P_i^2 + \beta_i P_i + \gamma_i, \quad i = 1,2,...n \qquad (1)$$

In the formula, i is the set of subscripts of the virtual synchronous power supply, α, β, γ are the cost coefficients of the distributed power supply, and $C_i(P_i)$ is the i-th virtual power supply cost function. This paper takes a three-machine system as an example, and its corresponding operation curve is shown in Figure 1.

In this paper, taking the power setpoint parameter as an example, the optimal power setting value should satisfy the following two formulas:

$$P_{setop1} + P_{setop2} = P_{setop3} \quad (2)$$

$$L(P_{setop1}) = L(P_{setop2}) = L(P_{setop3}) \quad (3)$$

In the above equation, P_{setop} is the optimal power setting and L(P) is the marginal cost of the output power. When the equation (2) is satisfied (ie, the three points A, B, and C in Fig. 1(a) are translated to A, B, and C, respectively), the output power of each converter is equal to the set power. The grid frequency is adjusted to the rated value; when the formula (3) is satisfied (ie, the three points D, E, and F in Fig. 1(b) are converted to D, E, and F), the corresponding power generation margin of each distributed power source The same cost value, independent micro-grid has the highest overall efficiency, at this time the cost of secondary frequency modulation is the lowest.

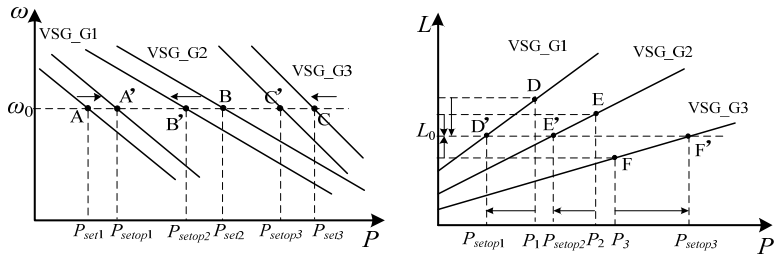

(a)Frequency droop curve (*b*) Marginal cost curve

Figure 1 Distributed power supply operating characteristics

2.2Secondary Consistency Strategy of Island Micro-grid Based on Distributed Consistency

Based on the above-mentioned secondary control principle, if the secondary regulation cost of the island microgrid system is taken into account, the total power generation cost is mainly considered from the distributed power supply side, and the reactive power cost is smaller than the active cost, so this section ignores reactive power. The cost mainly considers the cost of active power and the total power generation cost of the system is as follows [2]:

$$C_{\text{total}} = \sum_{i=1}^{n} C_i(P_i) = \sum_{i=1}^{n} (\alpha_i P_i^2 + \beta_i P_i + \gamma_i) \quad (4)$$

The secondary control objectives can be expressed as follows:

$$\begin{cases} \min \sum_{i=1}^{n} C_i(P_i) \\ \text{s.t} \sum_{i=1}^{n} P_i = P_{\text{Ld}} \\ P_{\min i} \le P_i \le P_{\max i} \end{cases} \quad (5)$$

In the above formula, P_i^{min} and P_i^{max} are power upper and lower limits respectively, and PLD is normal load power.

In order to increase the reliability of the secondary frequency modulation strategy and reduce the computational burden on the controller, this paper proposes a secondary frequency modulation strategy for islanding microgrid based on the distributed consensus algorithm [3].

In this paper, based on the discrete consensus algorithm of the new distributed frequency adjustment strategy, the overall control block diagram shown in Figure 2.

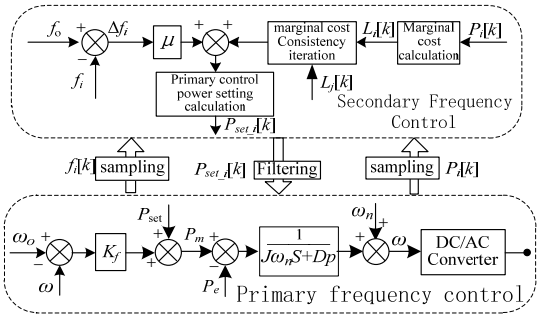

Figure. 2 Secondary frequency modulation control diagram based on distributed control

As shown in FIG. 2, the implementation steps of the distributed secondary frequency modulation strategy are as follows: Suppose that during the k-th sampling, the VSG i acquires its own output power $P_i[k]$, and calculates its own marginal cost according to the following formula:

$$\begin{cases} L_i[k] = \dfrac{d(C_i(P_i))}{dt} = \beta_i + 2\alpha_i P_i[k], \ i = 1,2,...,n \end{cases} \qquad (6)$$

In the formula, $P_i[k]$ is the power value at time k and $L_i[k]$ is the target marginal cost value of DGi at time k. After the calculation process is over, DG_i sends the marginal cost information to its neighbor DG_j, $j\varepsilon N_i$, and N_i is DGi's neighbor number set [4]. The calculated marginal cost is placed in the marginal cost state variable L_i [0], and then the marginal cost information is exchanged with the neighboring DG, and the consistency algorithm is used to calculate $L_i[k+1]$ as follows:

$$L_i[k+1] = \sum_{j \in \mathbf{N}_i} d_{ij} L_j[k] \qquad (7)$$

In the formula, d_{ij} is the update weight between DG_i and DG_j, which is related to the topology of the communication network. The above information interaction and consistency iterations are repeated until convergence converges to the average marginal cost Lave. According to equation (8), the target active power setting $P_{set\_i}[k]$ at time k is obtained and output to the local primary controller for secondary frequency control.

$$P_{set\_i}[k] = \begin{cases} \dfrac{L_{\text{ave}} + \mu \Delta f_i - \beta_i}{2\alpha_i} \\ \Delta f_i = f_{\text{o}} - f_i \end{cases} \qquad (8)$$

fo is the rated frequency and $\Delta f_i[k]$ is the local frequency deviation. μ is the feedback coefficient, which affects the distribution of the eigenvalues of the overall transfer matrix of the system. The larger the μ, the faster the convergence of the marginal cost. $P_{set\_i}[k]$ is the power setting at time k. It is noteworthy that when the power setting value obtained by the calculation of (8) exceeds the upper and lower limit constraints, the power is set according to the upper and lower limits [5].

When the (k+1) th sampling is performed, the steps (6), (7) and (8) are repeated, and the power setting value Pset is updated once every cycle is completed. After stabilization, the system satisfies equations (2) and (3) and achieves secondary control that takes into account economics.

3 Simulation Analysis

3.1 simulation environment to build

After modelling photovoltaic power generation systems, fuel cell power generation systems, lithium battery energy storage systems, micro gas turbines, and power electronic converters, an isolated island operation microgrid simulation model was built in Matlab/Simulink as shown in Figure 3 to verify the proposed Control Strategy.

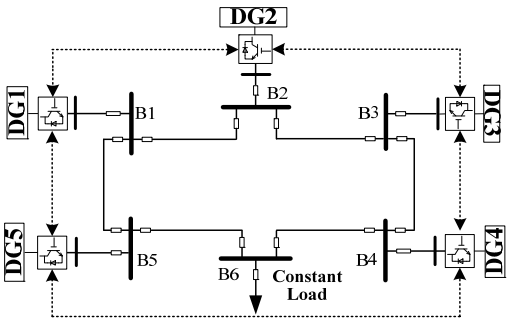

Fig. 3 Island Microgrid Simulation Model

The cost coefficients of the distributed units are shown in Table 1, and the control parameters and system circuit parameters are shown in Table 2. The model selects the ring network communication topology, so the construction consistency iteration matrix D is as follows:

$$\boldsymbol{D}=\begin{bmatrix} 1/5 & 1/5 & 0 & 1/5 & 1/5 \\ 1/5 & 1/5 & 1/5 & 0 & 1/5 \\ 1/5 & 1/5 & 1/5 & 1/5 & 0 \\ 0 & 1/5 & 1/5 & 1/5 & 1/5 \\ 1/5 & 0 & 1/5 & 1/5 & 1/5 \end{bmatrix} \tag{9}$$

Table 1 Cost Factors for Distributed Generations

coefficient	DG1	DG2	DG3	DG4	DG5
α/(\$/kW^{2}h)	0.02	0.013	0.012	0.01	0.05
β/(\$/kWh)	0.2	0.16	0.15	0.1	0.2
γ/(\$/h)	0.04	0.014	0.015	0.0015	0.012

Table 2 Microgrid System and Control Parameters

coefficient	Value	coefficient	Value
Rated voltage /V	380	B1-B5impedance/Ω	0.13+j0.016
Rated frequency /Hz	50	B4-B6impedance/Ω	0.1+j0.016
Filter capacitor /uF	150	Constant load /kW	50
Filter inductance /mH	5	The sampling period /ms	5
DG-Bus impedance/Ω	0.1+j0.013	K_f Value	13089
B1-B2 impedance /Ω	0.05+j0.01	K_v Value	3214
B2-B3 impedance /Ω	0.1+j0.016	J Value	8
B5-B6 impedance /Ω	0.08+j0.009	D_p Value	9
B3-B4 impedance /Ω	0.12+j0.009	μValue	0.5

3.2 Simulation Verification and Analysis

3.2.1 Primary Control Strategy Effectiveness Analysis

The constant power load PLD is 100 kW at the initial time, and the power setting values of DG1, DG2, DG3, DG4, and DG5 are 12 kW, 10 kW, 10 kW, 10 kW, and 10 kW, respectively. The virtual reactance is taken as 4mH. After the primary control strategy is started, each distributed power converter takes the load power according to the active set value, and the DG1 sets a large power, so the distribution is large and the rest is the same. After 2 s, the constant power load suddenly increases by 20 kW. Similarly, the increased power is distributed by each converter in proportion, as shown in FIG. 4. At this time, since the primary control is differential, the frequency after the system is stable is less than 50 Hz, and when the load increases, the frequency continues to decrease, as shown in FIG. 5.

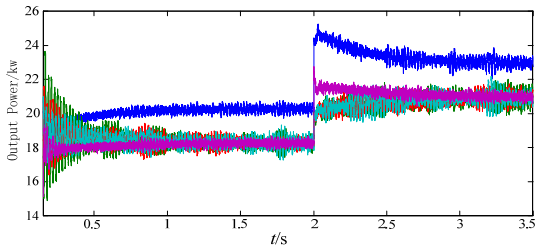

Figure 4 Output power of each converter Figure

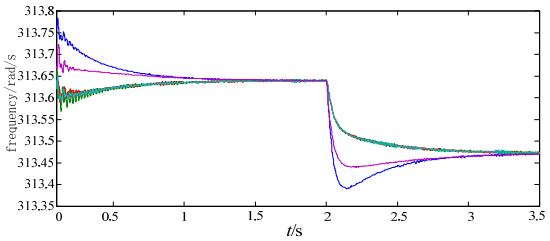

Figure 5 Real-time frequency detection of each node

In order to compare the advantages of improved droop control in primary control, this paper compares it with the traditional droop control without virtual reactance. Under the same simulation environment and parameters, it is shown in Figure 6. It can be seen from the figure that each converter is A small oscillation occurs before the output power is stable, and the adjustment time becomes longer. The same damping reduction can also be found from the real-time monitoring of frequency in FIG 7. Therefore, improved droop control increases the same damping and improves system stability. In addition, due to the increase of the virtual inertia, after a sudden change in load, it is stable after about 1 s, preventing the effect of rapid frequency fluctuation on system stability.

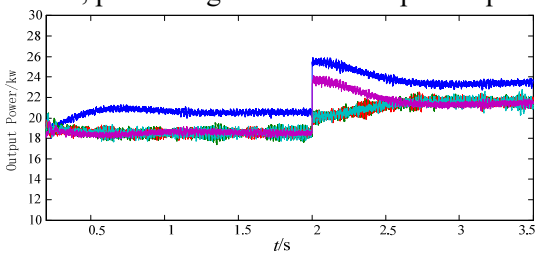

Figure 6 Output power of each converter

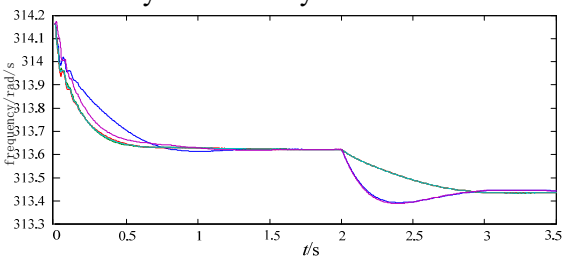

Figure 7 Real-time frequency detection of each node

3.2.2 Cost-effective secondary strategy effectiveness analysis

The simulation environment is the same. After starting the primary control strategy, each distributed power converter assumes the load power according to the active set value. After 1.2s, a secondary control strategy was initiated, the power setpoint of each unit was updated to the optimal value in real time, and the constant power load was increased by 20kW after 3s. The output power and node frequency of each unit are shown in Fig. 8 and shown in Fig. 9.

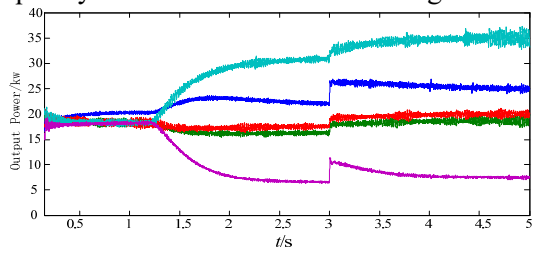

Figure 8 Output power of each converter

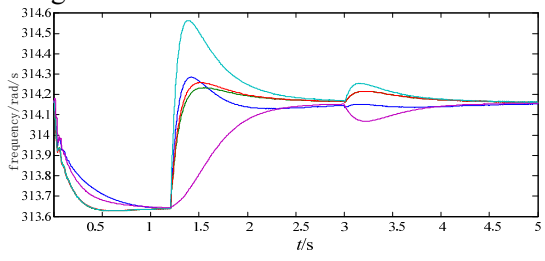

Figure 9 Real-time frequency detection of each node

As can be seen from the above figure, before the secondary strategy is started, since the sum of the power setting value of the power generating unit is less than the total load power setting value, the system frequency is lower than the rated value, and the unit output power of the same power setting value is equal. After the secondary frequency modulation strategy is started, the output power of each unit is different. The higher the cost is, the smaller the allocated power is, avoiding free adjustment of

active power output due to frequency fluctuation of each power generation unit, and less adjustment cost. It is worth noting that at this time, each distributed power source participates in the frequency adjustment and restores the frequency to the rated value. In the FM process, the distributed consensus algorithm dynamically finds the consistent marginal cost of each unit and changes the power setpoint in real time, as shown in FIGS. 10 and 11.

From the simulation waveforms, it can be seen that the proposed new distributed two-stage frequency modulation strategy has better dynamic and steady-state performance.

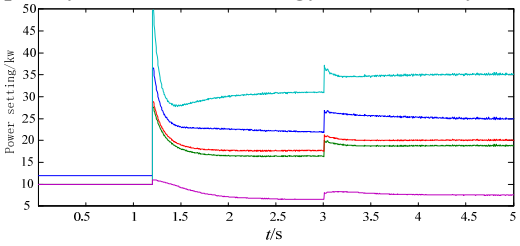

Figure 10 Primary Control Power Settings

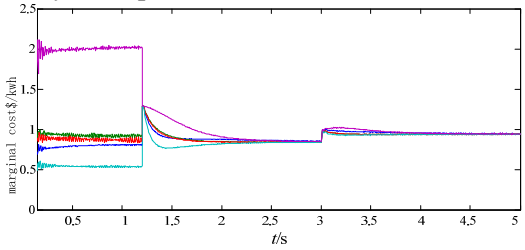

Figure 11 The distributed power marginal cost values

4. Conclusions

For the impedance characteristics of low-voltage microgrid line impedance and the strong coupling of active and reactive power control, a primary frequency control strategy for islanding microgrid based on non-communication interconnection is designed here, by using the traditional droop control method. The improved droop control with virtual inertia and virtual impedance is proposed as a primary control strategy to solve the problems of underdamping and low inertia of the island microgrid system and improve the stability of the system. In addition, taking the rapidity and economical efficiency of isolated microgrid as the goal, considering the difference of source, load, and storage frequency, a second-level frequency control strategy for islanding microgrid based on distributed control is proposed. In order to optimize the source, the load, and the storage to participate in the active power of the isolated microgrid frequency modulation, the purpose of the cooperative optimization of frequency modulation is achieved. The simulation results verify the stability of the actual operation effect of the proposed control strategy.

References

[1] M. Yazdanian, A. Mehrizi-Sani. Distributed control techniques in microgrids [J]. IEEE Transactions on Smart Grid,2014,5(6): 2901-2909

[2] Xu Y, Liu W, Gong J. Stable multi-agent-based load shedding algorithm for power systems[J]. IEEE Transactions on Power System,2011,26(4):2006-2014

[3] Chen F, Chen M, Li Q, et al. Multiagent-based reactive power sharing and control model for islanded microgrids[J]. IEEE Transaction on Sustainable Energy,2016,7(3):1232-1244

[4] Li Q, Chen F, Chen M, et al. Agent-based decentralized control method for islanded microgrids[J]. IEEE Transactions on Smart Grid,2016,7(2):637-949.

[5] Tang J, Liu J, Ponci F, et al. Adaptive load shedding based on combined frequency and voltage stability assessment using synchrophasor measurements[J]. IEEE Transactions on Power Systems, 2013, 28(2):2035-2047.